Demonstration of large peak-to-valley current ratios in InAs/AlGaSb/InAs single-barrier heterostructures

J. R. Söderström,[a] D. H. Chow, and T. C. McGill
T. J. Watson, Sr., Laboratory of Applied Physics, California Institute of Technology, Pasadena, California 91125

(Received 24 April 1989; accepted for publication 19 July 1989)

We report large peak-to-valley current ratios in InAs/$Al_xGa_{1-x}Sb$/InAs single-barrier tunnel structures. The mechanism for single-barrier negative differential resistance (NDR) has been proposed and demonstrated recently. A peak-to-valley current ratio of 3.4 (1.2) at 77 K (295 K), which is substantially larger than what has been previously reported, was observed in a 200-Å-thick $Al_{0.42}Ga_{0.58}Sb$ barrier. A comparison with a calculated current-voltage curve yields good agreement in terms of peak current and the slope of the NDR region. The single-barrier structure is a candidate for high-speed devices because of expected short tunneling times and a wide NDR region.

Double-barrier tunnel devices with negative differential resistance (NDR) have been the subject of great interest for several years.[1,2] New devices such as field-effect transistors with NDR,[3] the Stark effect transistor,[4,5] the resonant hot-electron transistor,[6] and devices for multiple level logic[7,8] are based on the double-barrier structure. High-speed devices such as oscillators and detectors for the THz range have also been made.[9] These devices are all based on the NDR in the current-voltage (I-V) characteristic of the tunnel structure.

Recently we proposed a new tunnel device in which NDR occurs in a single-barrier structure.[10,11] The NDR in this structure occurs because of the alignment of the bands in the barrier and contact layers and has a completely different origin than in the double-barrier case. A number of material systems have the required band structures and offsets to display this effect, including HgCdTe/CdTe, InAs/AlGaSb, and perhaps InAs/ZnTe.

Single-barrier structures are interesting for devices for several reasons. In double barrier structures the electrons tunnel through a quantum state with a width that will govern the tunneling time. In single barrier structures the electrons are not captured in such a quantum state which could yield faster tunneling times (good for high-speed operations). The NDR region is predicted to be much wider on the voltage scale than in the case of double barriers. This is of importance for high-frequency oscillators where the output power is governed by the product $\Delta I \times \Delta V$, where ΔI and ΔV are the width of the NDR region on the current and voltage scale, respectively.

The single-barrier NDR has experimentally been demonstrated by a few groups. The first observation was made in 1987 by Chow *et al.* in a single-barrier HgCdTe heterostructure.[12] In 1988 Munekata *et al.* observed NDR in an InAs/$Al_{0.4}Ga_{0.6}Sb$/InAs (200 Å barrier) structure.[13] A peak-to-valley current ratio (P/V ratio) of ~ 1.1 was obtained at 77 K. Recently Beresford *et al.* reported room-temperature NDR in an InAs/$Al_{0.5}Ga_{0.5}Sb$/InAs (150 Å barrier) structure.[14]

In this study we have investigated NDR in InAs/$Al_xGa_{1-x}Sb$/InAs single-barrier structures with 200-Å-thick barriers. P/V ratios as high as 1.2 and 3.4 at room temperature and 77 K, respectively, have been observed for an aluminum concentration of 42%. The 77 K value of 3.4 is substantially larger than what has previously been reported for any single-barrier structure. We also report a wide NDR region (~ 140 meV). Six single-barrier samples were grown with aluminum concentrations in the barrier ranging from 38% to 48%. Four of the samples yielded NDR. We have compared our results to a simple theoretical calculation.

A qualitative understanding of the single-barrier NDR can be obtained by considering the positions of the conduction- and valence-band edges under applied bias as shown in Fig. 1. From the Wentzel–Kramers–Brillouin approximation theory we know that an electron traveling in the z direction has a probability of tunneling through the barrier given by the transmission coefficient

$$T \propto \exp\left(-2\int_0^w K\,dz\right),$$

where K is the imaginary wave vector (or the decay constant) in the band gap of the barrier and w is the thickness of the barrier. K can be obtained from a two-band model, $k\cdot p$ theory calculation.[15] The important thing about the two-band model is that it accounts for the reduction of the decay constant for energies closer to the valence band, re-

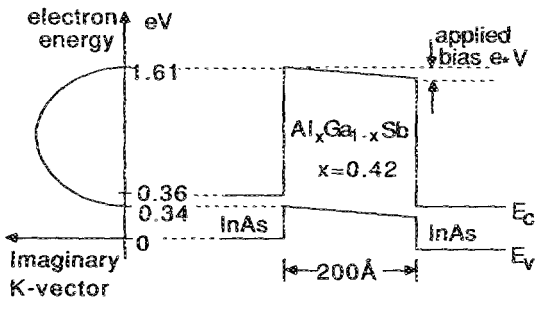

FIG. 1. Band-edge diagram (Γ point) for the single-barrier structure under applied bias. The imaginary wave vector in the barrier layer is plotted as function of the electron energy. NDR occurs due to the enhanced tunneling probability for electrons close to the valence band of the barrier layer.

[a] On leave from Chalmers University of Technology, Department of Physics, S-412 96 Göteborg, Sweden.

sulting in a maximum of K at (or close to) midgap of the barrier layer as shown in the left-hand side of Fig. 1. The requirement for getting NDR in a single-barrier structure is that the tunneling electrons (at low voltages) are injected close to the valence band of the barrier layer where the decay constant is small. As the voltage increases the electrons tunnel at higher average energies in the barrier, resulting in larger K, smaller transmission coefficient and hence a lower current. It should be emphasized that this effect can be seen only in single-barrier structures where the electrons tunnel below midgap (or below the maximum of the imaginary wave vector) of the barrier. This explains why GaAs/AlGaAs single-barrier structures do not display this effect.

The samples were grown in a Perkin–Elmer 430 molecular beam epitaxy (MBE) system. An As cracker and an Sb cracker were used to produce dimers instead of tetramers in the molecular beams. Details of bulk growth parameters for InAs and GaSb can be found elsewhere.[16] Calibrations of growth rates and x values were done with reflection high-energy electron diffraction (RHEED) oscillations and bulk film thickness measurements.

The single-barrier structures were grown on GaAs (100) substrates. Due to the large lattice mismatch (7.2%) between the substrate and the epilayer, a thick buffer layer was grown. The buffer layer consisted of 5000 Å GaAs grown at 600 °C, a five-period $In_{0.7}Ga_{0.3}As$/GaAs (2 monolayers/2 monolayers) superlattice grown at 500–520 °C, and 1.5 μm InAs (heavily Si doped) grown at 500 °C. The superlattice at the GaAs/InAs interface reduces the number of strain-induced dislocations which penetrate into the InAs layer.[16,17] The single-barrier structures were grown at 500 °C on top of the buffer layers. Each structure consisted of a 200 Å undoped $Al_xGa_{1-x}Sb$ ($38\% \leqslant x \leqslant 48\%$) barrier sandwiched between 100 Å undoped InAs spacer layers and 500 Å lightly doped ($n = 2\times10^{16}$ cm^{-3}) InAs spacer layers. The two-step spacer layer technique is used to reduce the number of Si donors in the barrier region and has previously been used for double-barrier structures.[18] Finally a 2500-Å-thick heavily doped ($n = 2\times10^{18}$ cm^{-3}) InAs cap layer was grown.

Mesa structures with varying areas (down to 100 μm^2) were prepared using standard photolithography and liftoff techniques. The evaporated Au/Ge contacts served as masks during etching in H_2SO_4:H_2O_2:H_2O (1:8:80) for 90 s, which resulted in $\sim$0.7 μm high mesas. Au/Ge deposited on the etched InAs buffer layer was used as the back contact. No annealing was necessary since Au/Ge forms an ohmic contact to InAs. The mesas were probed with a thin gold wire to establish electrical contact to the devices.

Figure 2 shows an experimentally obtained current density versus voltage (J-V) characteristic for a single-barrier structure with a 200-Å-thick $Al_{0.42}Ga_{0.58}Sb$ barrier. NDR can be seen at room temperature and 77 K for both positive and negative bias. The remainder of the discussion focuses on the reverse bias peak (i.e., electrons injected from the top mesa contact) since it gave the best result. The P/V ratios are as high as 1.2 and 3.4 at room temperature and 77 K, respectively. The 77 K value is the largest P/V ratio ever reported for single-barrier structures. The peak current densities are 30 A/cm^2 at 295 K and 22 A/cm^2 at 77 K. The width of the NDR region at 77 K is about 140 mV.

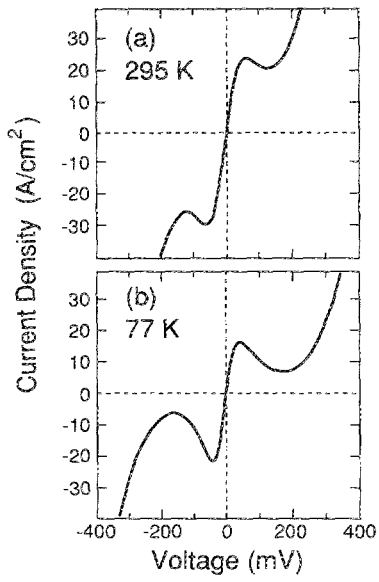

FIG. 2. Experimental J-V characteristic at (a) room temperature and (b) 77 K for a 200-Å-thick $Al_{0.42}Ga_{0.58}Sb$ single-barrier enclosed by InAs. The device size is $10\times10\,\mu m^2$. The P/V ratios (in reverse bias) are as high as 1.2 and 3.4 at 295 and 77 K, respectively.

Figure 3 shows the calculated J-V curve for the same structure. Details of the calculations have been reported earlier.[19] A peak at $\sim$15 mV followed by a wide region of NDR can be seen. The peak current density is $\sim$20 A/cm^2 which is only slightly smaller than the measured value. The measured peak voltage is about twice as large as the calculated peak voltage which could be atrributed to series resistance in the circuit which has not been accounted for in the calculation. The slope of the NDR region is about 200 Ω^{-1} cm^{-2} which is close to the 350 Ω^{-1} cm^{-2} value that was obtained from the theoretical curve.

Obviously the calculated and experimental curves are in good agreement in several respects. This is in contrast to

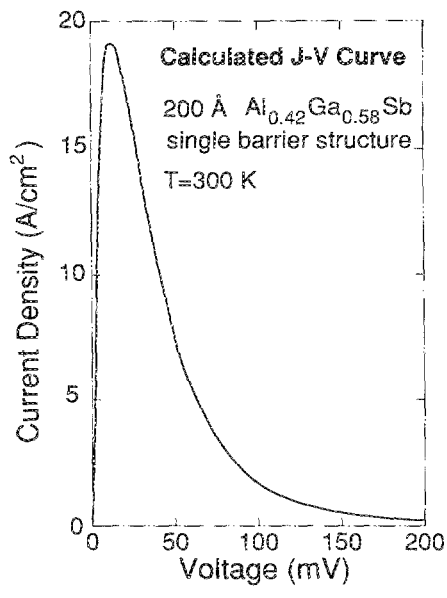

FIG. 3. Calculated J-V curve at 300 K for the single-barrier structure.

previous studies. The computer program does not account for any other current transport mechanism than elastic tunneling of electrons. We will briefly discuss possible additional current transport mechanisms that could account for the measured excess valley current. Since the barrier in the conduction band is high (1.3 eV), thermionic currents over the barrier will only give a small current contribution at low voltages. However, at higher voltages the potential drop over the undoped layer on the emitter side will result in electrons being ballistically injected close to or above the top of the barrier, producing a larger current. In the valence band, thermally excited holes are present (due to the small band gap of InAs) which do not experience any barrier and give rise to a hole current. Furthermore, electrons occupying valence-band states will start to tunnel over to states in the conduction band when the voltage over the barrier aligns the energy of these states. Other possible current mechanisms include inelastic tunneling processes and currents on the mesa surface. The calculated J-V curve indicates that much better P/V ratios can be obtained if the excess currents can be reduced. We are presently working to achieve this goal.

NDR was observed in three more samples with the aluminum concentrations of 44, 40, and 38%. P/V ratios in these samples were smaller than 1.5. At an aluminum concentration of 38% the single-barrier structure may be semimetallic according to reported values of band gaps and offsets.[20,21] The fact that NDR is observed anyway can be explained either by an error in the growth rate calibration or by error in the band offsets. Even if the calibration and the offset values are correct we might still be able to explain the NDR due to the fact that when a bias is applied to the semimetallic structure the barrier region gets skewed and the valence-band state of the barrier layer gets quantized. These states will no longer extend out in the InAs conduction band and the incoming electrons will experience a barrier exactly as in the case of higher x values.

The samples with 44% and 46% aluminum concentration have some interesting features. The 46% sample shows no NDR at any temperature. However, a room-temperature inflection in the I-V curve can clearly be seen. This inflection disappears as the temperature is lowered, and at 77 K the curve is exponential as in the case of thermionic emission currents over a barrier. We attribute this effect to an increase in the energy difference between the conduction band of the contact layer and the valence band of the barrier (due to the increase of the InAs and AlGaSb band gaps). Thus, the tunneling probability is reduced at 77 K. The same argument holds for the behavior of the 44% sample in which no NDR is observed at 77 K. As the temperature is increased to ~180 K a NDR region with a ratio P/V of 1.1 appears. As the temperature is increased even further, the NDR disappears due to thermionic currents.

To summarize, we have observed NDR in InAs/AlGaSb/InAs single-barrier structures with substantially larger P/V ratios than previously reported. The measured J-V curve is in close agreement with the theoretically obtained curve in terms of peak current density, peak voltage, and the slope of the NDR region. The result of the calculation also shows that much larger P/V ratios can be obtained if the excess currents can be controlled. Other experiments to examine the physics of these structures are in progress.

We acknowledge the support of the Air Force Office of Scientific Research under grant No. 86-0306. Two of us (JRS and DHC) are thankful for financial support from the Sweden–America Foundation and TRW, respectively.

[1] L. L. Chang, L. Esaki, and R. Tsu, Appl. Phys. Lett. **24**, 593 (1974).
[2] J. R. Söderström and T. G. Andersson, Superlatt. Microstruct. **5**, 109 (1989).
[3] T. K. Woodward, T. C. McGill, H. F. Chung, and R. D. Burnham, Appl. Phys. Lett. **51**, 1542 (1987).
[4] A. R. Bonnefoi, D. H. Chow, And T. C. McGill, Appl. Phys. Lett. **47**, 888 (1985).
[5] F. Beltram, F. Capasso, S. Luryi, S. N. G. Chu. A. Y. Cho, and D. L. Sivco, Appl. Phys. Lett. **53**, 219 (1988).
[6] T. Futatsugi, Y. Yamaguchi, K. Imamura, S. Muto, N. Yokoyama, A. Shibatomi, Jpn. J. Appl. Phys. **26**, L131 (1987).
[7] S. Sen, F. Capasso, A. Y. Cho, and D. Sivco, IEEE Trans. Electron Devices **34**, 2185 (1987).
[8] J. R. Söderström and T. G. Andersson, IEEE Electron Device Lett. **9**, 200 (1988).
[9] T. C. L. G. Sollner, W. D. Goodhue, P. E. Tannenwald, C. D. Parker, and D. D. Peck, Appl. Phys. Lett. **43**, 588 (1983).
[10] D. H. Chow and T. C. McGill, Appl. Phys. Lett. **48**, 1485 (1986).
[11] G. A. Sai-Halasz, R. Tsu, and L. Esaki, Appl. Phys. Lett. **30**, 651 (1977).
[12] D. H. Chow, T. C. McGill, I. K. Sou, J. P. Faurie, and C. W. Nieh, Appl. Phys. Lett. **52**, 54 (1988).
[13] H. Munekata, T P. Smith III, and L. L. Chang, J. Vac. Sci. Technol. B **7**, 324 (1989).
[14] R. Beresford, L. F. Luo, W. I. Wang, Appl. Phys. Lett. **54**, 1899 (1989).
[15] E. O. Kane, *Physics of III-V compounds* (Academic, New York, 1966), Vol. 1, Chap. 3, pp. 75–100.
[16] J. R. Söderström, D. H. Chow, and T. C. McGill, *Proceedings of the MRS 1989 Spring Meeting, San Diego* (Materials Research Society, Pittsburgh, in press).
[17] S. Kalem, J. I. Chyi, and H. Morkoç, Appl. Phys. Lett. **53**, 1648 (1988).
[18] C. I. Huang, M. J. Paulus, C. C. Bozada, S. C. Dudley, K. R. Evans, C. E. Stutz, R. L. Jones, and M. E. Cheney, Appl. Phys. Lett. **51**, 121 (1987).
[19] A. R. Bonnefoi, D. H. Chow, and T. C. McGill, J. Appl. Phys. **62**, 3836 (1987).
[20] G. J. Gulatieri, G. P. Schwarz, R. G. Nuzzo, and W. A. Sunder, Appl. Phys. Lett. **49**, 1073 (1986).
[21] G. J. Gulatieri, G. P. Schwarz, R. G. Nuzzo, R. J. Malik, and J. F. Walker, J. Appl. Phys. **61**, 5337 (1987).